NOAA Technical Memorandum NESS 50

U.S. DEPARTMENT OF COMMERCE
National Oceanic and Atmospheric Administration
National Environmental Satellite Service

An Examination of Tropical Cloud Clusters Using Simultaneously Observed Brightness and High Resolution Infrared Data From Satellites

ARNOLD GRUBER

WASHINGTON, D.C.
tember 1973

NOAA TECHNICAL MEMORANDA

National Environmental Satellite Service Series

The National Environmental Satellite Service (NESS) is responsible for the establishment and operation of the National Operational Meteorological Satellite System and of the environmental satellite systems of NOAA. The three principal offices of NESS are Operations, Systems Engineering, and Research.

NOAA Technical Memoranda NESS series facilitate rapid distribution of material that may be preliminary in nature and may be published formally elsewhere at a later date. Publications 1 through 20 and 22 through 25 are in the former series, ESSA Technical Memoranda, National Environmental Satellite Center Technical Memoranda (NESCTM). The current series, NOAA Technical Memoranda, National Environmental Satellite Service (NESS), includes 21, 26, and subsequent issuances.

Publications listed below are available from the National Technical Information Service, U.S. Department of Commerce, Sills Bldg., 5285 Port Royal Road, Springfield, Va. 22151. Price: $3.00 paper copy; $0.95 microfiche. Order by accession number, when given, in parentheses.

ESSA Technical Memoranda

NESCTM 15 Some Aspects of the Vorticity Structure Associated With Extratropical Cloud Systems. Harold J. Brodrick, Jr., May 1969. (PB-184-178)

NESCTM 16 The Improvement of Clear Column Radiance Determination With a Supplementary 3.8μ Window Channel. William L. Smith, July 1969. (PB-185-065)

NESCTM 17 Vidicon Data Limitations. Arthur Schwalb and James Gross, June 1969. (PB-185-966)

NESCTM 18 On the Statistical Relation Between Geopotential Height and Temperature-Pressure Profiles. W. L. Smith and S. Fritz, November 1969. (PB-189-276)

NESCTM 19 Applications of Environmental Satellite Data to Oceanography and Hydrology. E. Paul McClain, January 1970. (PB-190-652)

NESCTM 20 Mapping of Geostationary Satellite Pictures--An Operational Experiment. R. C. Doolittle, C. L. Bristor, and L. Lauritson, March 1970. (PB-191-189)

NESCTM 22 Publications and Final Reports on Contracts and Grants, 1969--NESC. January 1970. (PB-190-632)

NESCTM 23 Estimating Mean Relative Humidity From the Surface to 500 Millibars by Use of Satellite Pictures. Frank J. Smigielski and Lee M. Mace, March 1970. (PB-191-741)

NESCTM 24 Operational Brightness Normalization of ATS-1 Cloud Pictures. V. R. Taylor, August 1970. (PB-194-638)

NESCTM 25 Aircraft Microwave Measurements of the Arctic Ice Pack. Alan E. Strong and Michael H. Fleming, August 1970. (PB-194-588)

NOAA Technical Memoranda

NESS 21 Geostationary Satellite Position and Attitude Determination Using Picture Landmarks. William J. Dambeck, August 1972. (COM-72-10916)

NESS 26 Potential of Satellite Microwave Sensing for Hydrology and Oceanography Measurements. John C. Alishouse, Donald R. Baker, E. Paul McClain, and Harold W. Yates, March 1971. (COM-71-00544)

NESS 27 A Review of Passive Microwave Remote Sensing. James J. Whalen, March 1971. (COM-72-10546)

NESS 28 Calculation of Clear-Column Radiances Using Airborne Infrared Temperature Profile Radiometer Measurements Over Partly Cloudy Areas. William L. Smith, March 1971. (COM-71-00556)
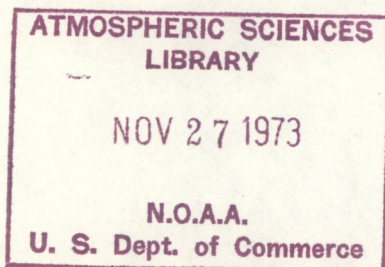
U.S. DEPARTMENT OF COMMERCE
National Oceanic and Atmospheric Administration
National Environmental Satellite Service

NOAA Technical Memorandum NESS 50

AN EXAMINATION OF TROPICAL CLOUD CLUSTERS USING SIMULTANEOUSLY OBSERVED BRIGHTNESS AND HIGH RESOLUTION INFRARED DATA FROM SATELLITES
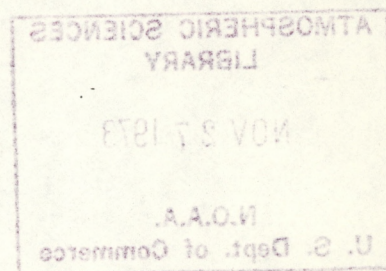
Arnold Gruber

NOAA

WASHINGTON, D.C.
September 1973

UDC 551.576.1:551.521.32:535-1:551.507.362.2(213)

53		Physics
535-1		Infrared radiation
551.5		Meteorology
.507		Instrument carriers
	.362.2	Satellites
.521		Radiation
	.32	Reflected or emitted radiation
.576		Clouds
	.1	Cloud structure and formations

CONTENTS

AN EXAMINATION OF TROPICAL CLOUD CLUSTERS USING SIMULTANEOUSLY OBSERVED BRIGHTNESS AND HIGH RESOLUTION INFRARED DATA FROM SATELLITES

Arnold Gruber
National Environmental Satellite Service, NOAA
Washington, D.C.

ABSTRACT. In an attempt to infer the convective activity of tropical cloud clusters, a study was made of simultaneous observations of infrared (10 to 12 μm) and reflected energy (0.55 to 0.75 μm) measured by the scanning radiometer flown aboard the NOAA 1 satellite. The brightest areas were not always coincident with the coldest areas. Correlation coefficients between equivalent blackbody temperatures and brightnesses were computed for five different ranges of brightness. The highest brightness ranges were poorly correlated with the equivalent blackbody temperatures. These results suggest that brightness enhancing techniques alone may not be adequate for the study of convective activity in cloud clusters.

INTRODUCTION

Recently, attention has been directed to brightness enhancement techniques as a means of identifying deep cumulonimbus clouds associated with tropical cloud clusters. The enhancement procedures can be applied digitally (Martin and Suomi 1972) or by analog devices (Woodley et al. 1972). The working hypothesis is that the cumulonimbus clouds, being deeper than the surrounding clouds, will appear brighter when enhanced and will thus be easily identified. However, for a given solar zenith angle, the optical thickness determines the amount of incident solar energy reflected from clouds. The optical thickness depends on the concentration and size of the cloud particles as well as the geometrical thickness.

Theoretical and observational studies of layer clouds (Nieburger 1949, Twomey et al. 1967, Griggs 1968, Danielson et al. 1969) have shown that clouds less than 1 km thick can reflect 80 percent or more of the incident solar radiation. These studies, which generally are concerned with low-level stratus clouds, have also indicated that this is close to the maximum albedo for the cloud layer. Thus, further increases in the thickness of the clouds produce little change in the albedo. In figure 1, the cloud albedo is plotted as a function of cloud thickness for various combinations of liquid water content and absorbing and nonabsorbing conditions (conservative scattering). Solid curves correspond to a liquid water content of 0.40 g m^{-3}, and the dashed curves to 0.20 g m^{-3}. Of each pair of curves, the right hand member represents conservative scattering and left hand member a fractional absorption per scattering of 1.2×10^{-3}. θ_o is the zenith angle of the incident

energy and μ_0 is the cosine of the zenith angle. Horizontal bars are Neiburger's (1949) experimental results (with standard deviations). (After Twomey et al. 1967.) Also included are Nieburger's (1949) observational results. The important point is that at a cloud thickness of about 700 m the cloud albedo is close to its maximum value. Taking the above into account, one must consider whether enhanced or very bright features can adequately represent deep convective towers. It is also desirable to determine if there is any relation between brightness and the heights of clouds.

To provide some insight into these questions, simultaneous observation of infrared (10 to 12 μm), and reflected energy (0.55 to 0.75 μm) have been studied for selected cloud clusters in the tropical Pacific Ocean. The working hypothesis is that if the clouds that appear brightest in the visible range are truly the deep penetrative convective clouds, they should also exhibit rather low brightness temperatures in the infrared. Under reasonable assumptions, the infrared temperatures can be related to cloud top heights (Koffler et al. 1972). Thus, a study of simultaneously observed brightness and equivalent blackbody temperatures will provide clues to the heights of cloudy areas. At this point we actually are obtaining a minimum height curve for a given brightness level. This occurs because a high thin cloud will be partially transparent to infrared radiation and so will appear to have a temperature representative of a lower-than-actual height. This was discussed by Fritz and Rao (1967). When dealing with the lowest temperatures, this ambiguity obviously will not pose any great difficulties.

DATA

The data upon which the analysis is based were obtained with the scanning radiometer flown aboard the NOAA 1 satellite. Both the visible (0.55 to 0.75 μm) and infrared (10 to 12 μm) data were obtained for June 25, 1971. They are archived on a National Meteorological Center grid with 1024 points to a grid square. The infrared observations have a resolution of about 7 km and the visible about 3.5 km at the subsatellite point. The sensing instrument is collinear, i.e., the signal is received at the spacecraft through the same sight, then optically split, one part going to the visible radiometer and the other to the infrared radiometer. This results in a relative mapping error estimated to be about 1.5 km. This mapping error is important, because in an earlier attempt using infrared scanning radiometer data and advanced vidicon camera system data the relative mapping error was sufficiently large (>30 km) to make a detailed study of the convective scale impractical. The visible data for this study have been normalized using a procedure developed by Taylor (1970) and are in the form of digital counts ranging from 0 at the darkest end to 254 at the brightest end. The infrared data are archived as equivalent blackbody temperatures (believed to have a reliable range from about $330°$ to $184°K$) and have been corrected for limb-darkening (Koffler, personal communication). Since we are dealing in general with high clouds, the results will not be very sensitive to the limb-darkening correction used.

The infrared data suffer from noise in the system. The noise, expressed in terms of equivalent blackbody temperature, varies with scene temperature. Schwalb (1972) estimates the RMS noise to be 2°C at scene temperatures of

300°K and about 8°C at scene temperatures of 185°K.

The cases studied were selected by a subjective examination of images in both the infrared and visible portions of the spectrum. Figure 2 shows the locations of the cases selected. The small squares represent the NMC grid upon which the data are archived. Each grid is composed of a 32 x 32 set of data points, centered at the intersection of the grid lines.[1]

At the latitude where the five cases are located, each grid box is about 240 km on a side.

CORRELATION BETWEEN BRIGHTNESS AND TEMPERATURE

To examine the data for any relations between brightness and temperature (and thus height), correlation coefficients between the two were computed for the full brightness range and for the four separate brightness ranges, each being restricted to higher brightnesses (and thus greater cloudiness). The correlation coefficients were adjusted to take into account the effect of the RMS noise levels previously cited. The adjustments were made by assuming the RMS value of 8°C is applicable for all scene temperatures. (This tends to overestimate the correlation coefficients—a worst case situation.) The variance of temperature can be written as

$$\sigma_T^2 = \sigma_t^2 + \sigma_\epsilon^2 \qquad (1)$$

where σ_t^2 is the true variance and σ_ϵ^2 represents the noise contribution. Thus, the adjusted correlation coefficient is given as

$$R^* = \left[\frac{\sigma_T}{(\sigma_T^2 - \sigma_\epsilon^2)^{1/2}} \right] R \quad , \qquad (2)$$

where R is the correlation coefficient computed from the actual data. The results of the computations and other pertinent statistics are listed in table 1. The adjusted correlation coefficients vary between -0.55 and -0.84 when the full brightness range is used. However, as we restrict ourselves to higher brightness ranges the correlation coefficients become smaller; in two cases (5-42 and 20-55) they became essentially zero.

These results indicate that any relation between the brightest clouds and cloud heights is at best marginal. However, the higher correlations obtained when the full brightness range was used suggest that it may be possible to stratify the data into the broad categories of high-level clouds and low-level clouds. This could be useful when investigating deep convection.

The relations between brightness and temperature are illustrated by bivariate frequency distributions (figs. 3 to 7). In these figures the ordinate is in °K, the abscissa is the brightness class interval. The isopleths of

---

[1]Locations 5-42, 6-42, and 7-43 had some erroneous data resulting in data sets 32 x 27 for grids 5-42 and 6-42 and 32 x 28 for grid 7-43.

frequency have all been multiplied by 10. The brightness data were collected in 2°K class intervals. In general, the frequency distributions tend to show a rather broad spread of temperatures for a given brightness range, especially at higher brightness categories. For example, at brightness class 17 of location 19-55 (fig. 3) the temperature ranges from about 200° to 240°K. Using Jordan's (1958) mean tropical sounding, this corresponds to heights of about 10.5 to 16.5 km. And in most of the clusters studied there is generally more than one temperature mode for a given brightness class, particularly at high brightness levels. Thus, any unique relation between cloud top heights and brightness is quite difficult to establish.

The most straightforward interpretation is that the various temperature modes observed for a given brightness class represent clouds at different heights. However, other factors can account for the spread of temperature found in each brightness class. Among them are:

(1) Resolution. Since the resolution of the visible sensor is twice that of the infrared sensor it is possible for small bright areas to have relatively high temperatures associated with them. This condition is most likely when one is viewing cloud elements whose size is smaller than the resolving ability of the infrared instrument against a warm background such as the Earth's surface. This effect probably will be small for the cloud clusters considered here, because these clusters tend to be composed of fairly solid cloud cover. In these clusters, the convective cloud elements protrude above a background of thick middle to high clouds.

(2) System noise. The RMS noise of the instrument expressed in terms of equivalent blackbody temperature varies between 0.3°C at scene temperatures of 300°K, and 1.4°C at scene temperatures of 185°K. When ground handling of the data is considered, the estimates are about 2° and 8°C, respectively. These values, estimated by Schwalb (1972), represent the worst cases to be expected. These RMS noise values were for use with NOAA 2 data, but probably are valid for use with NOAA 1 data as well. This kind of temperature error probably can account for much of the observed dispersion. An attempt to adjust the correlation coefficients for the effects of noise has already been described. It will be seen later that the mapped infrared analysis is smooth over most of the field, suggesting that the effects of noise are small.

(3) Variations in emissivity. Variations in cloud emissivity may result in apparent temperature fluctuations without appreciable changes in brightness. This is the basis for the earlier statement that infrared temperatures yield, at best, a minimum height curve. In this analysis it was assumed that temperatures less than about 230°K are produced by clouds with emissivities nearly equal to 1.0. This temperature was selected because it is near the low temperature limit for supercooled water (Johnson 1954). Thus, clouds with temperatures of 230°K or less are undoubtedly ice clouds with tops at about 250 to 300 mb, i.e., either cirrus or tall cumulus clouds.

EXAMINATION OF MAPPED DATA

It is instructive to examine the spatial patterns exhibited by the two fields. For example, one would expect towers or groups of convective towers

to exhibit centers of low temperatures with sharp gradients surrounding them. If brightness-enhancing techniques are valid we would expect to find similar relations, i.e., high brightness areas surrounded by sharp gradients in brightness.

Some examples believed to represent deep penetrative "hot tower" convection are presented in figures 8 to 10. Temperature was analyzed every 10°K between 190° and 230°K and brightness was analyzed every 25 units between 150 and 250. In these diagrams the temperature and brightness contours are superimposed. To reduce some of the confusion generated by this type of display, these analyses include only temperature values of 230°K or less and brightness values of 150 or greater. In all the examples one should note the existence of the general inverse relation described in the discussion of the bivariate frequency analyses. However, the details are of primary interest, for that is where one would expect to find the evidence for "hot tower" convection. Although the detailed patterns are complicated, some of the more interesting features will be pointed out. Of particular interest are the areas labeled A, B, C, D, and E of cluster 20-55 (fig. 8). Area A shows much temperature detail within a larger cold region (T ≤ 210°K). The size of the region and the coherency of the isopleth pattern suggest that we are looking at a region of active hot towers. Also the brightest area is not coincident with the coldest region, a result that was unexpected. The difference in location is more than can be accounted for by relative mapping errors or differences in resolution. The reasons for these differences in location are not clear. However, since the data are collocated it seems likely that it can be attributed to physical causes. Areas D and E in the lower left corner of the grid show a relation to the brightest features similar to that in Area A.

Areas B and C were selected because they illustrate a peculiar phenomenon. Both show coherent low temperature centers (T ≤ 200°K). The Area B temperature minimum coincides perfectly with the brightness maximum, while the Area C temperature minimum is found in a relative brightness minimum!

The other cases (figs. 9 to 12) show similar characteristics. Locations 5-42 and 6-42 (figs. 10 and 11), however, contain good examples of the condition known as saturation. Saturation occurs when the reflected energy is greater than the observing system is capable of measuring; thus, it is indicative of the brightest region in the field of view. Within the saturated area there are no gradients of brightness. The areas marked "A" in figures 10 and 11 are saturated regions. In both cases the temperature analysis indicates considerable structure, permitting a more reliable interpretation of the cloud field than do the brightness data.

Saturation is a function of the observing system and occurs with the current satellite systems. Under these conditions, the brightness data will not be suitable for isolating details of convective activity.

ESTIMATING AMOUNT OF CONVECTIVE ACTIVITY

One of the goals of this analysis is to provide an estimate of the amount of deep penetrative convection occurring over a specified area. This is an important parameter in cumulus parameterization schemes (Kuo 1965).

I propose a procedure that utilizes both the infrared and visible data in an attempt to provide such estimates. It is similar to an earlier study (Gruber 1973) in which only infrared temperatures were used. It depends, principally, on locating a mode in the frequency distribution of infrared temperatures near the temperature of the level of zero buoyancy for undiluted parcel ascent. It is then assumed that temperatures less than or equal to that modal temperature are produced by penetrative convection. The brightness data are used to eliminate cirrus clouds, which often appear as low temperature, low brightness clouds. Good examples of the cirrus condition are shown in the lower right corner of figure 8 and the left side of figure 10, where temperatures of less than 230°K are associated with brightness values less than 150.

In the application of the procedure to the five cases studied, the level of zero buoyancy was taken to be 206°K (based on the sounding presented by Reed and Recker 1971)), and only the upper 25 percent of the brightness range was used. The estimated coverage (in percent) of the areas of hot tower convection, the modal temperatures near the levels of zero buoyancy, and the mean temperatures of all the data points are shown in table 2. The coverage varies between 2.2 and 18.6 percent. The 18.6-percent value appears somewhat high; however, it was situated in an area of very active convection, as suggested by the low mean temperature of 217°K. Also, the percent coverage is highly dependent on the size of the area under consideration.

It should be stressed that the proposed procedure and the resulting estimates are to be considered very tentative. The model upon which it depends does not take into account such potentially important factors as the stage of development of the convective elements and entrainment processes. Nor is there independent information on the size and location of the convective elements associated with the clusters studied, which makes verification of the estimates virtually impossible.

CONCLUDING REMARKS

The analysis of simultaneously observed infrared and brightness data over cloud clusters indicates a negative correlation between brightness and temperature. The correlations between -0.55 and -0.84 suggest that one could isolate, from brightness data alone, regions of cloud clusters where low temperature and deep convection should be expected. However, it is felt that the preceding analysis has shown that for isolating details of convective activity in tropical cloud clusters reliance on brightness alone can lead one astray.

The conclusions, however, are not completely unambiguous. There is the problem of different resolution between the visible and infrared channels, which may be ameliorated by the high resolution radiometer aboard the NOAA 2 satellite which has 0.5-n mi resolution for both infrared and visible data.

There is also the problem of variations of emissivity which make interpretation difficult. There is no apparent solution to this problem in the immediate future.

The most serious deficiency associated with the analysis, however, is the lack of ground truth data on how many convective cores there are, what their

heights and locations are, and whether or not they are precipitating. The lack of this information makes it difficult to establish on an absolute basis that either spectral region can be used to identify "hot towers" adequately. What can be said is that an analysis of high resolution infrared data collocated with simultaneous observations of reflected energy does not completely support the assertion that brightness enhancement procedures provide a suitable means of identifying "hot tower" convection.

The results of this analysis were also confusing in that coherent bright centers were often displaced from coherent low temperature centers, but not in any systematic fashion. Since the data are collocated, there must be a physical reason for the displacement.

Finally, the required ground truth that probably will be available from the GATE observations, and the higher resolution satellite data available from VHRR (and to be available from the proposed geostationary satellite, SMS), should make it possible to remove much of the uncertainty encountered in this analysis.

REFERENCES

Danielson, R. E., Moore, D. R., and Van de Hulst, H. C., "The Transfer of Visible Radiation Through Clouds," Journal of Atmospheric Sciences, Vol. 26, No. 5, Part 2, Sept. 1969, pp. 1078-1087.

Fritz, Sigmund and Rao, P. Krishna, "On the Infrared Transmission Through Cirrus Clouds and the Estimation of Relative Humidity From Satellites," Journal of Applied Meteorology, Vol. 6, No. 6, Dec. 1967, pp. 1088-1096.

Griggs, M., "Aircraft Measurements of Albedo and Absorption of Stratus Clouds, and Surface Albedo," Journal of Applied Meteorology, Vol. 7, No. 6, Dec. 1968, pp. 1012-1017.

Gruber, Arnold, "Estimating Rainfall in Regions of Active Convection," Journal of Applied Meteorology, Vol. 12, No. 1, Feb. 1973, pp. 110-118.

Johnson, John C., Physical Meteorology, John Wiley and Sons, New York, 1954, 393 pp.

Jordan, Charles L., "Mean Soundings for the West Indies Area," Journal of Meteorology, Vol. 15, No. 2, Feb. 1958, pp. 91-97.

Koffler, Russell, Decotiis, Arthur G., and Rao, P. Krishna, "A Procedure for Estimating Cloud Amount and Height From Satellite Infrared Radiation Information," Monthly Weather Review, Vol. 101, No. 3, Mar. 1973, pp. 240-243.

Kuo, H. L., "On Formation and Intensification of Tropical Cyclones Through Latent Heat Release by Cumulus Convection," Journal of Atmospheric Sciences, Vol. 22, No. 1, Jan. 1965, pp. 40-63.

Martin, David W., and Suomi, Verner E., "A Satellite Study of Cloud Clusters Over the Tropical North Atlantic Ocean," Bulletin of the American Meteorological Society, Vol. 53, No. 2, Feb. 1972, pp. 135-156.

Neiburger, M., "Reflection, Absorption and Transmission of Insolation by Stratus Cloud," Journal of Meteorology, Vol. 6, No. 2, Apr. 1949, pp. 98-104.

Reed, Richard J., and Recker, Ernest E., "Structure and Properties of Synoptic-Scale Wave Disturbances in the Equatorial Western Pacific," Journal of Atmospheric Sciences, Vol. 28, No. 7, Oct. 1971, pp. 1117-1133.

Schwalb, Arthur, "Modified Version of the Improved TIROS Operational Satellite (ITOS D-G)," NOAA Technical Memorandum NESS 35, U.S. Department of Commerce, National Environmental Satellite Service, Washington, D.C., Apr. 1972, 48 pp.

Taylor, Ray V., "Operational Brightness Normalization of ATS-1 Cloud Pictures," ESSA Technical Memorandum NESCTM 24, U.S. Department of Commerce, National Environmental Satellite Service, Washington, D.C., Aug. 1970, 15 pp.

Twomey, Sean, Jacobowitz, Herbert, and Howell, Hugh B., "Light Scattering by Cloud Layers," Journal of Atmospheric Sciences, Vol. 24, No. 1, Jan. 1967, pp. 70-79.

Woodley, William L., Sancho, Briseida, and Miller, Alan H., "Rainfall Estimation From Satellite Cloud Photographs," NOAA Technical Memorandum ERL OD-11, Experimental Meteorology Laboratory, Boulder, Colo., Feb. 1972, 43 pp.

Table 1.--Correlation coefficients and other pertinent statistics for the 5 cases studied. From the left, the columns list the location and number of the grid, the brightness range for which statistics were computed, the number of observations, the mean brightness, the variance of the brightness, the mean temperature, the temperature range, the variance of the temperature, and the adjusted correlation coefficient.

Grid	Bright. range	No. of obs.	Mean bright.	Bright variance σ^2 B	Mean temp. °K	Temp. range °K	Temp. variance σ^2 T	Adj.* corr. coef.
5-42	0-254	864	172	4173	234	196-296	383	-0.77
4.6N	50-254	810	182	3055	231	196-292	270	- .66
147.9W	100-254	698	197	1652	229	196-278	211	- .55
	150-254	598	209	867	226	196-278	159	- .39
	200-254	338	229	278	223	196-262	138	- .10
6-42	0-254	864	198	1512	229	188-264	192	-0.84
6.5N	50-254	864	198	1515	229	188-264	192	- .84
149W	100-254	845	200	1333	229	188-264	187	- .83
	150-254	754	208	802	227	188-260	169	- .80
	200-254	449	226	276	222	188-250	120	- .68
7-43	0-254	896	194	2641	235	196-288	327	-0.80
	50-254	890	195	2499	235	196-284	318	- .79
7.7N	100-254	831	202	1807	233	196-282	266	- .73
146.3W	150-254	706	216	898	229	196-278	201	- .58
	200-254	497	231	287	226	196-272	156	- .38
20-55	0-254	1024	175	2066	228	188-270	282	-0.55
10.6N	50-254	1024	175	2066	228	188-270	282	- .55
107.6W	100-254	952	180	1679	226	188-270	272	- .55
	150-254	690	200	763	223	188-260	253	- .38
	200-254	321	223	242	201	188-254	218	- .06
19-55	0-254	1024	217	848	217	186-260	215	-0.67
	50-254	1024	217	848	217	186-260	215	- .67
9.5N	100-254	1024	218	790	217	186-260	208	- .65
109.5W	150-254	994	219	612	217	186-256	190	- .58
	200-254	750	229	242	213	186-244	142	- .30

*Adjustment based on a RMS noise of 8K

Table 2.--Estimated percent of area covered by active convection, mean temperature in °K, and modal temperatures near the level of zero buoyancy (LZB) for each case.

Grid	Percent coverage	Mean temp. (°K)	Modal temp. near LZB (°K)
5-42	1.7	234	206
6-42	5.3	229	206
7-43	2.4	235	206
20-55	7.2	235	206
19-55	18.6	217	204
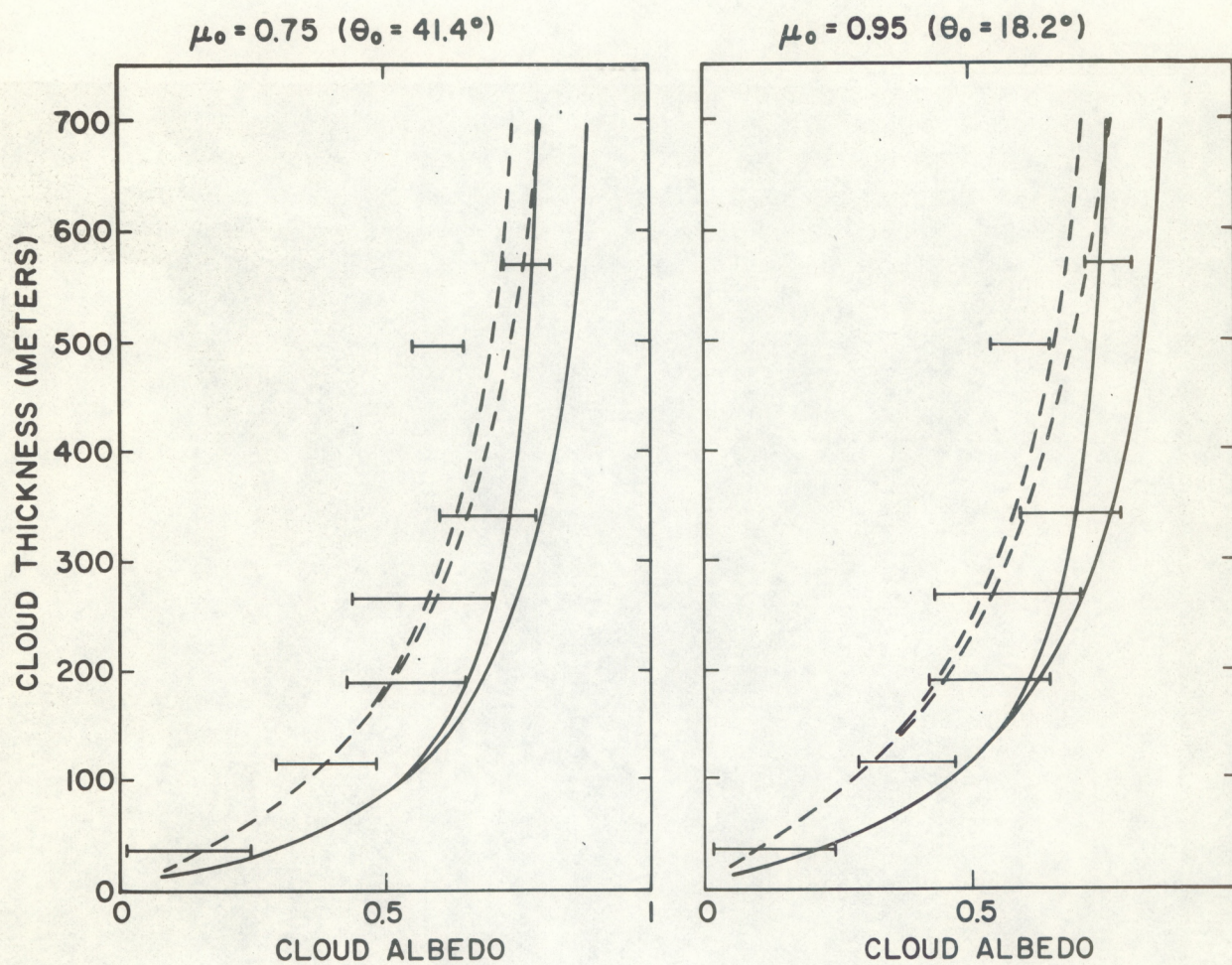
Figure 1.--Cloud albedo vs. cloud thickness.

12
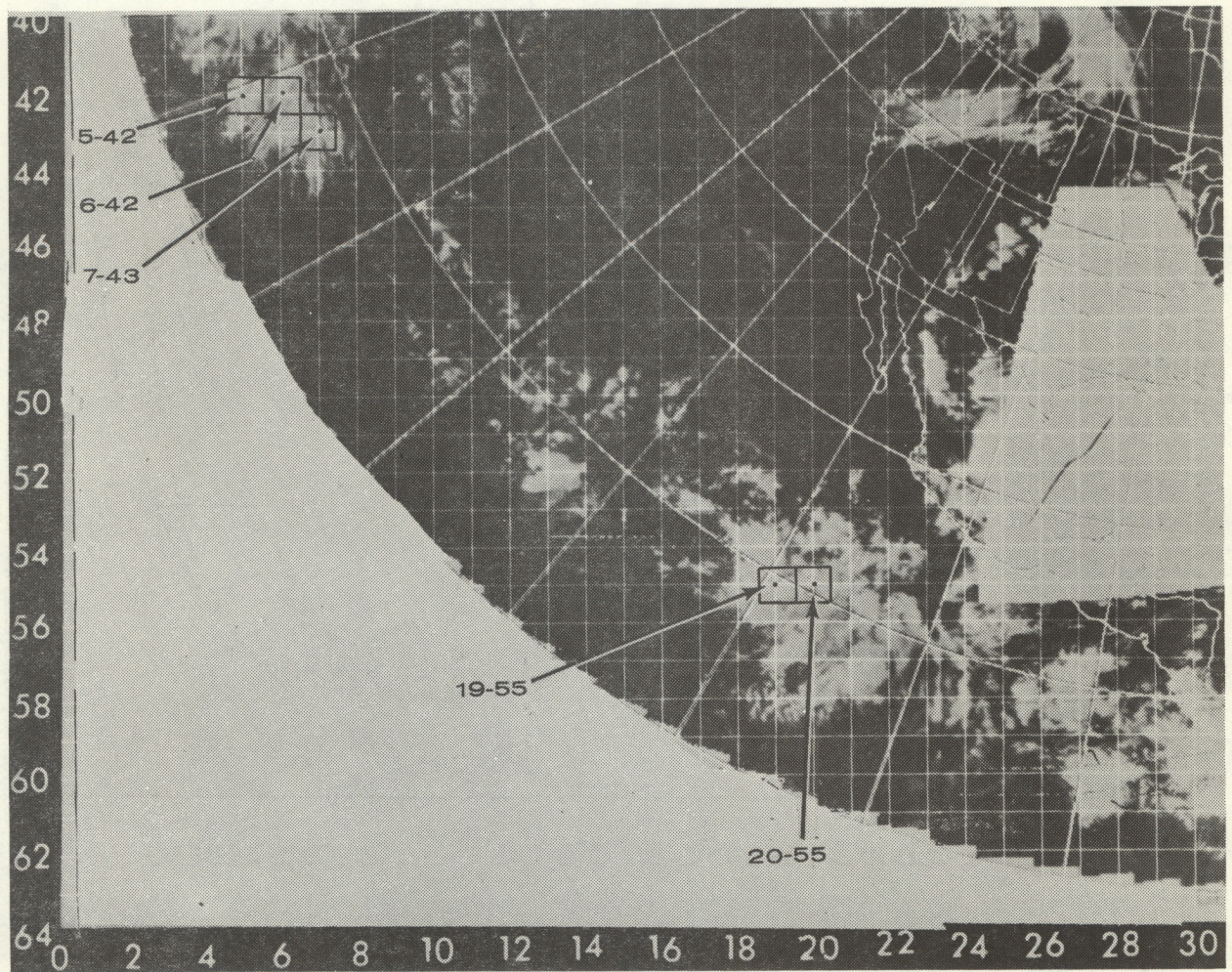
Figure 2.--Location of the areas of the cloud clusters selected for study.
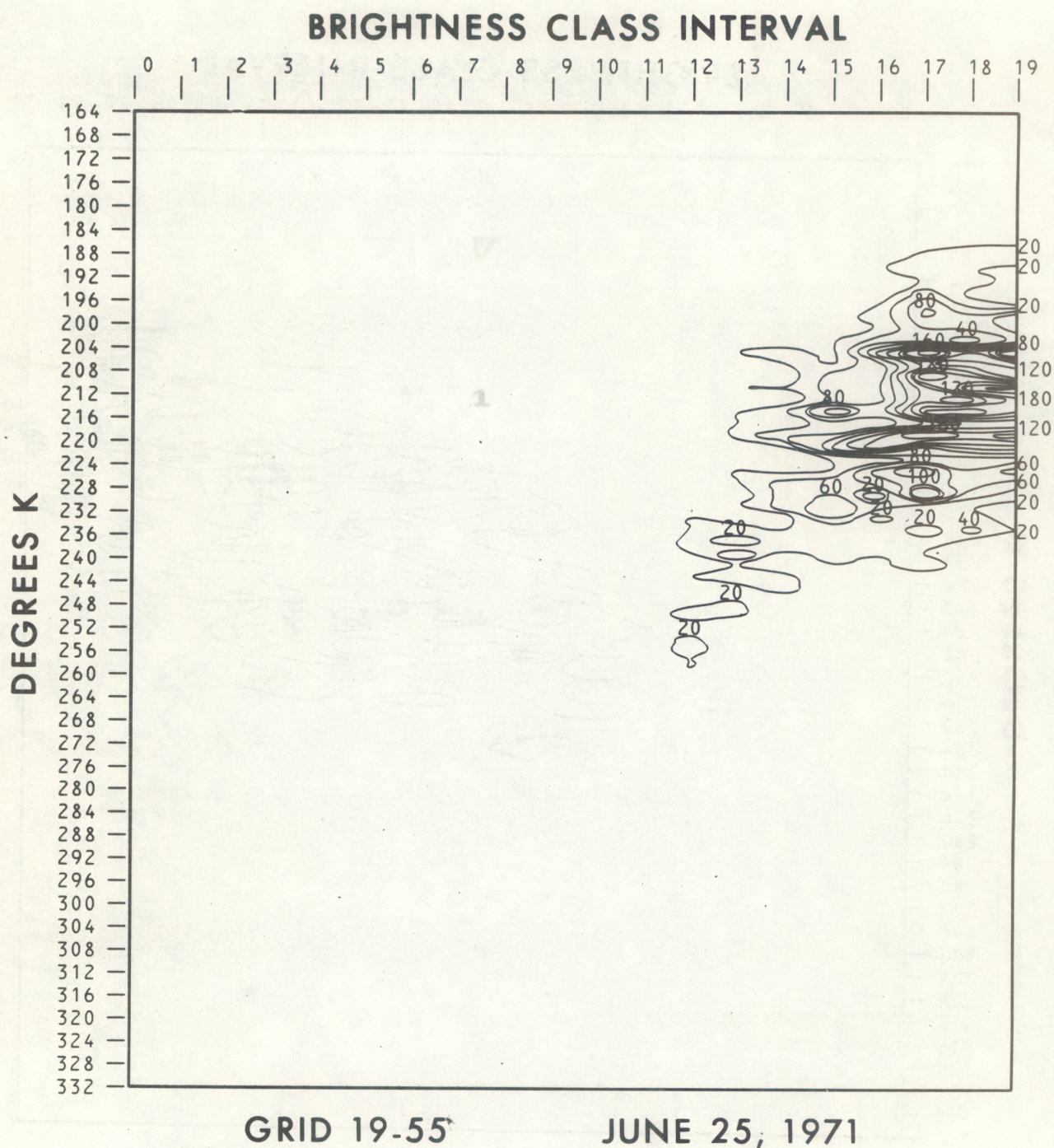
Figure 3.--Bivariate frequency distribution for location 19-55.

BRIGHTNESS CLASS INTERVAL
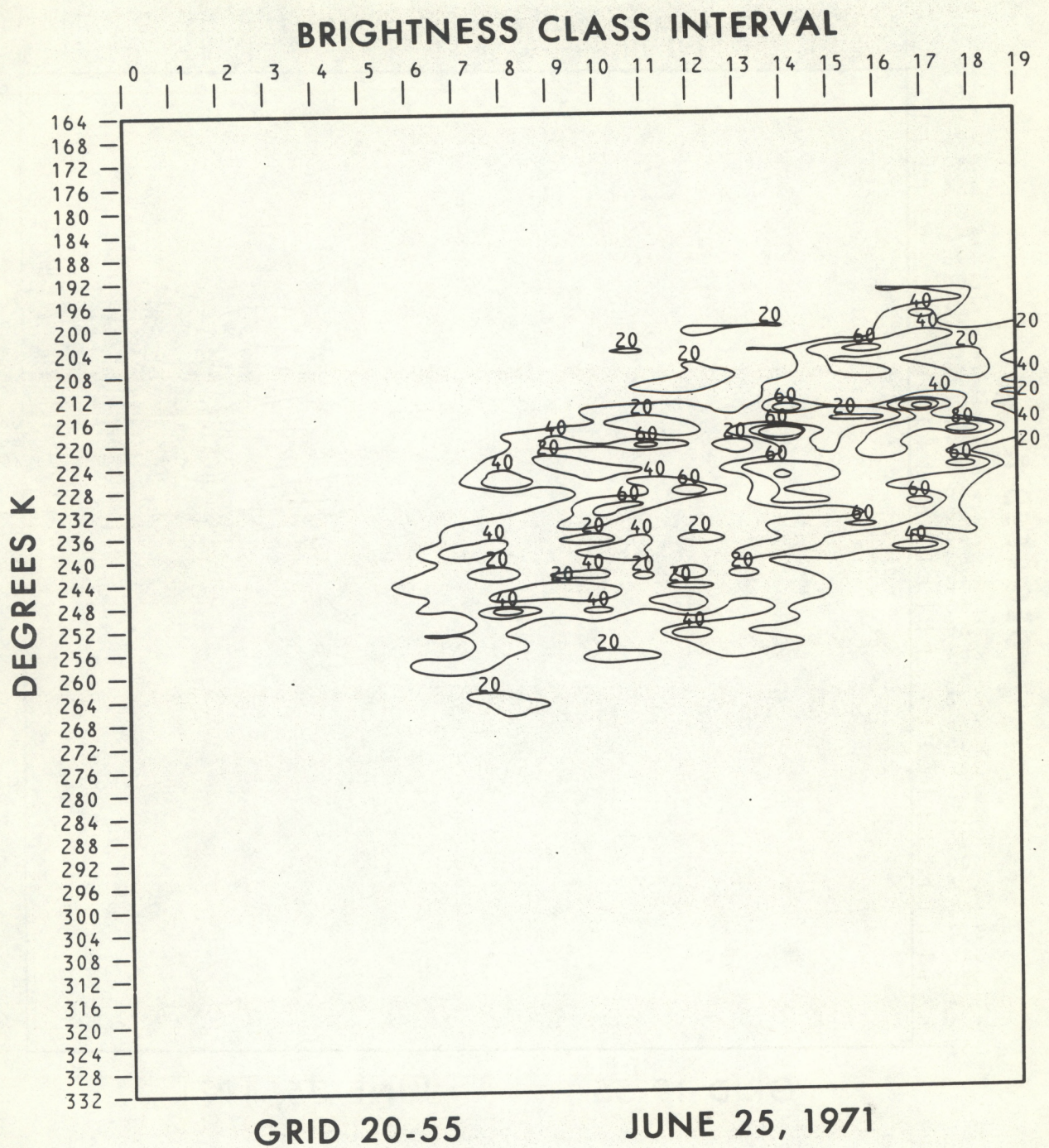
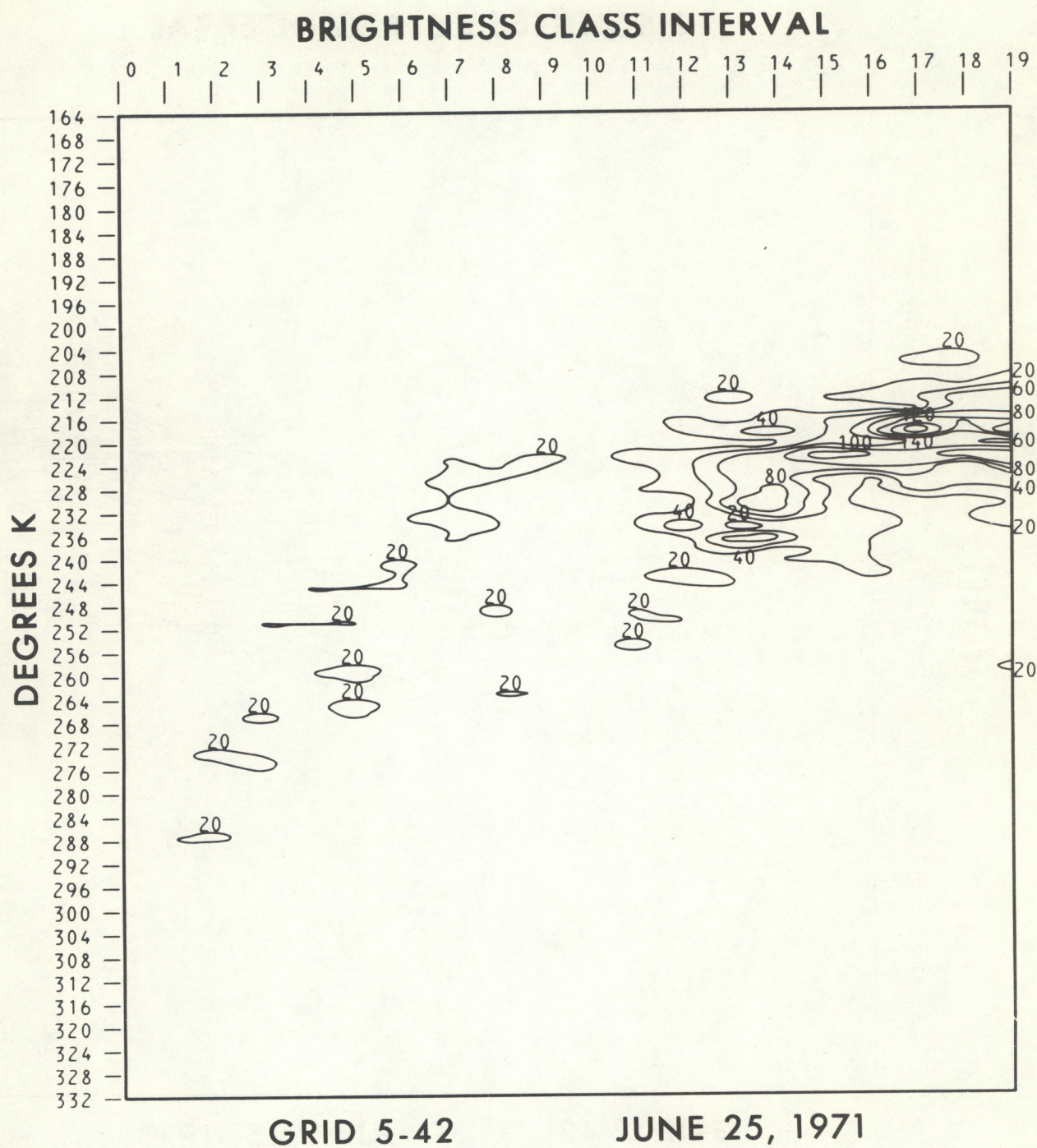Figure 4.--Bivariate frequency distribution for location 20-55.

BRIGHTNESS CLASS INTERVAL
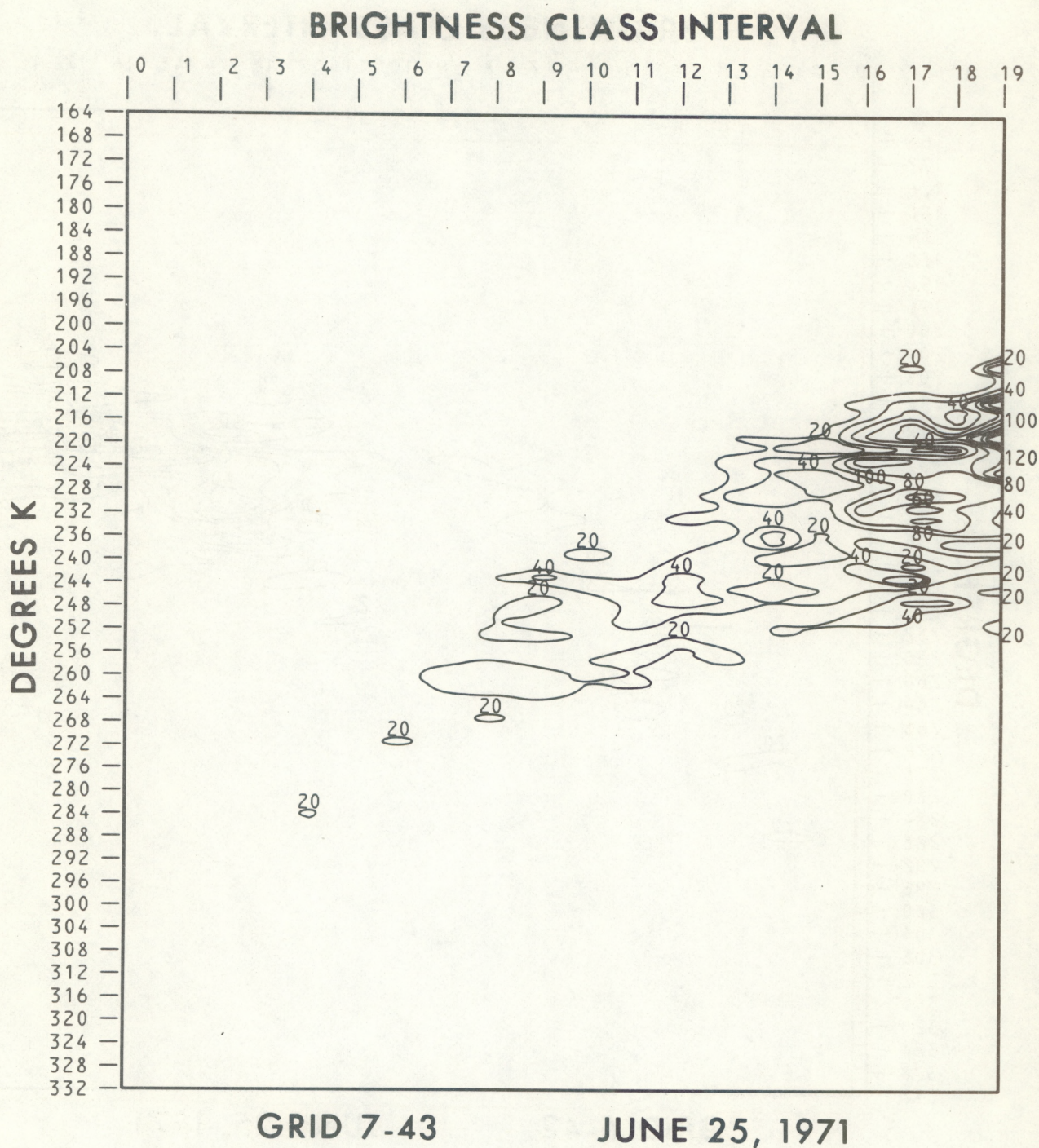
Figure 5.--Bivariate frequency distribution for location 7-43.

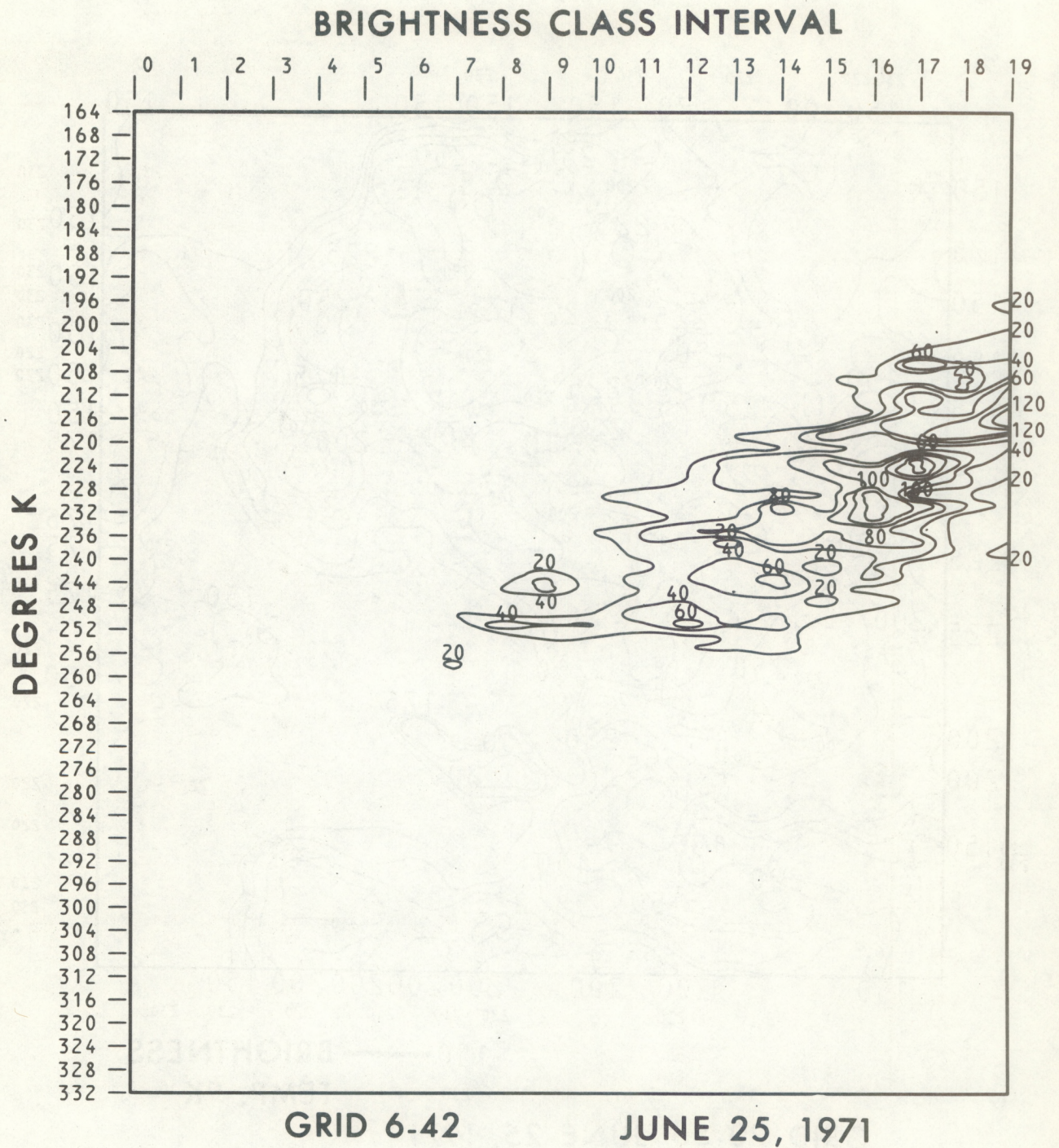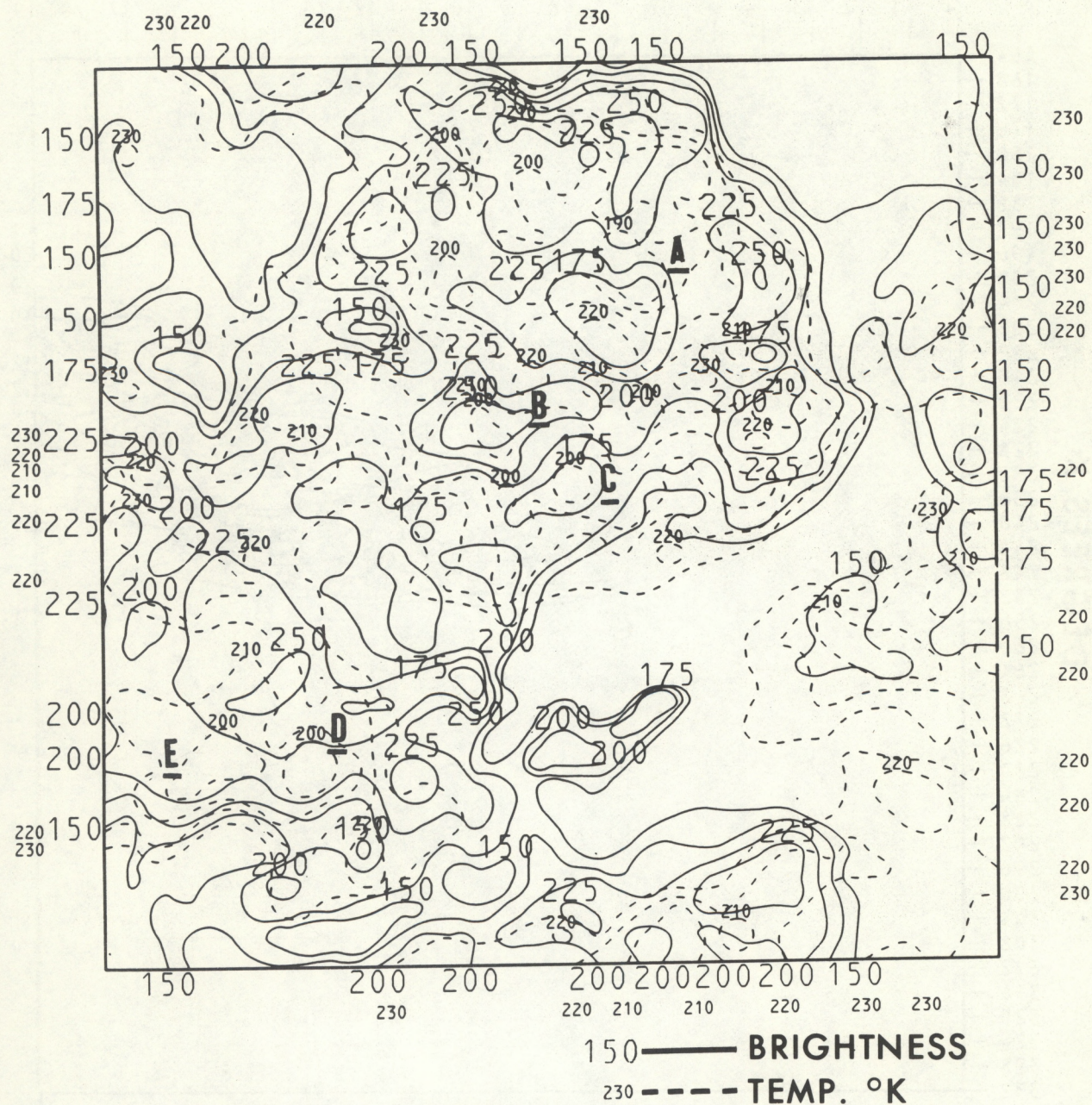Figure 6.--Bivariate frequency distribution for location 5-42.

BRIGHTNESS CLASS INTERVAL

Figure 7.--Bivariate frequency distribution for location 6-42.

GRID 20-55 JUNE 25, 1971

Figure 8.--Analyzed map of infrared temperatures (dashed)
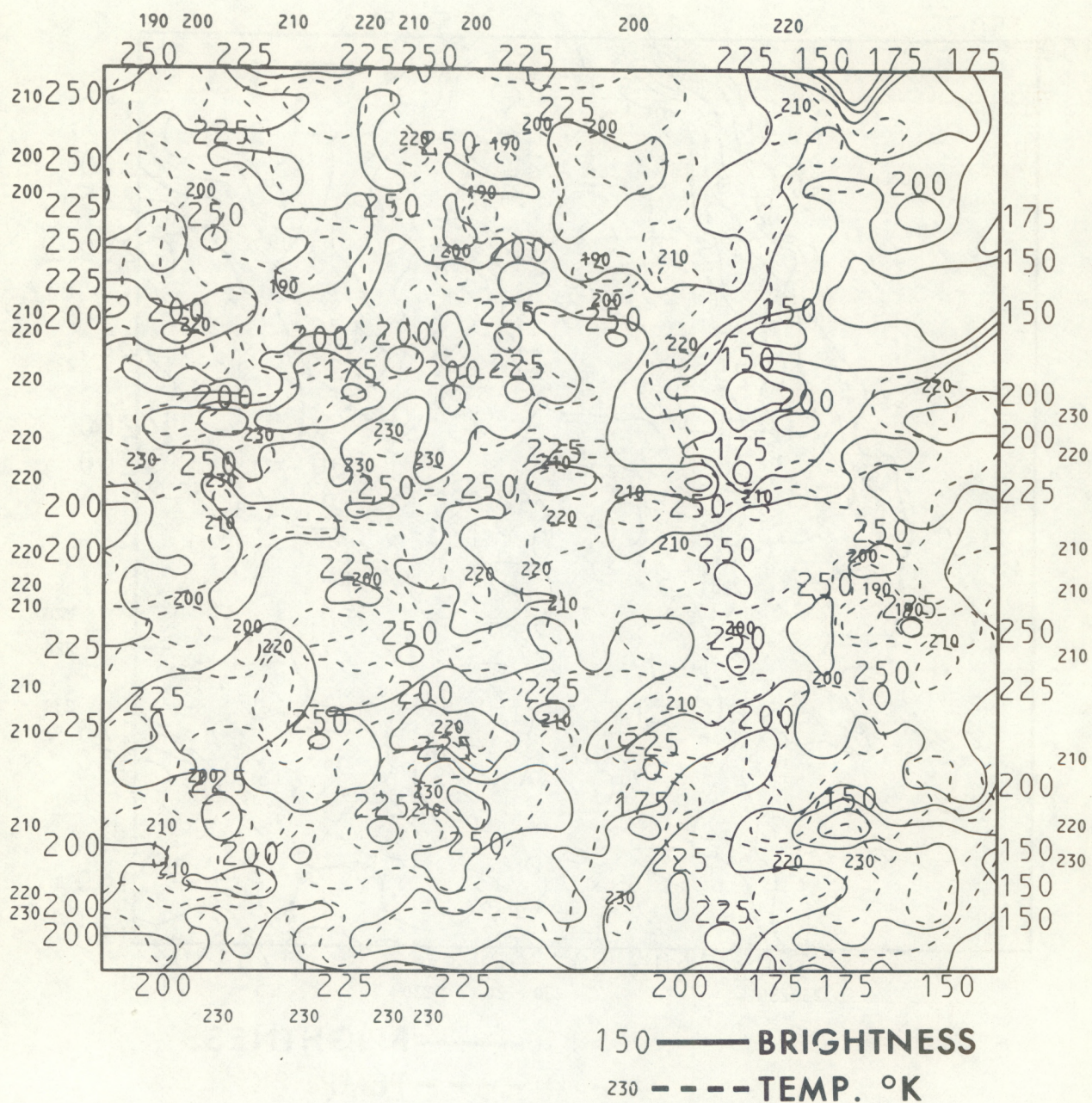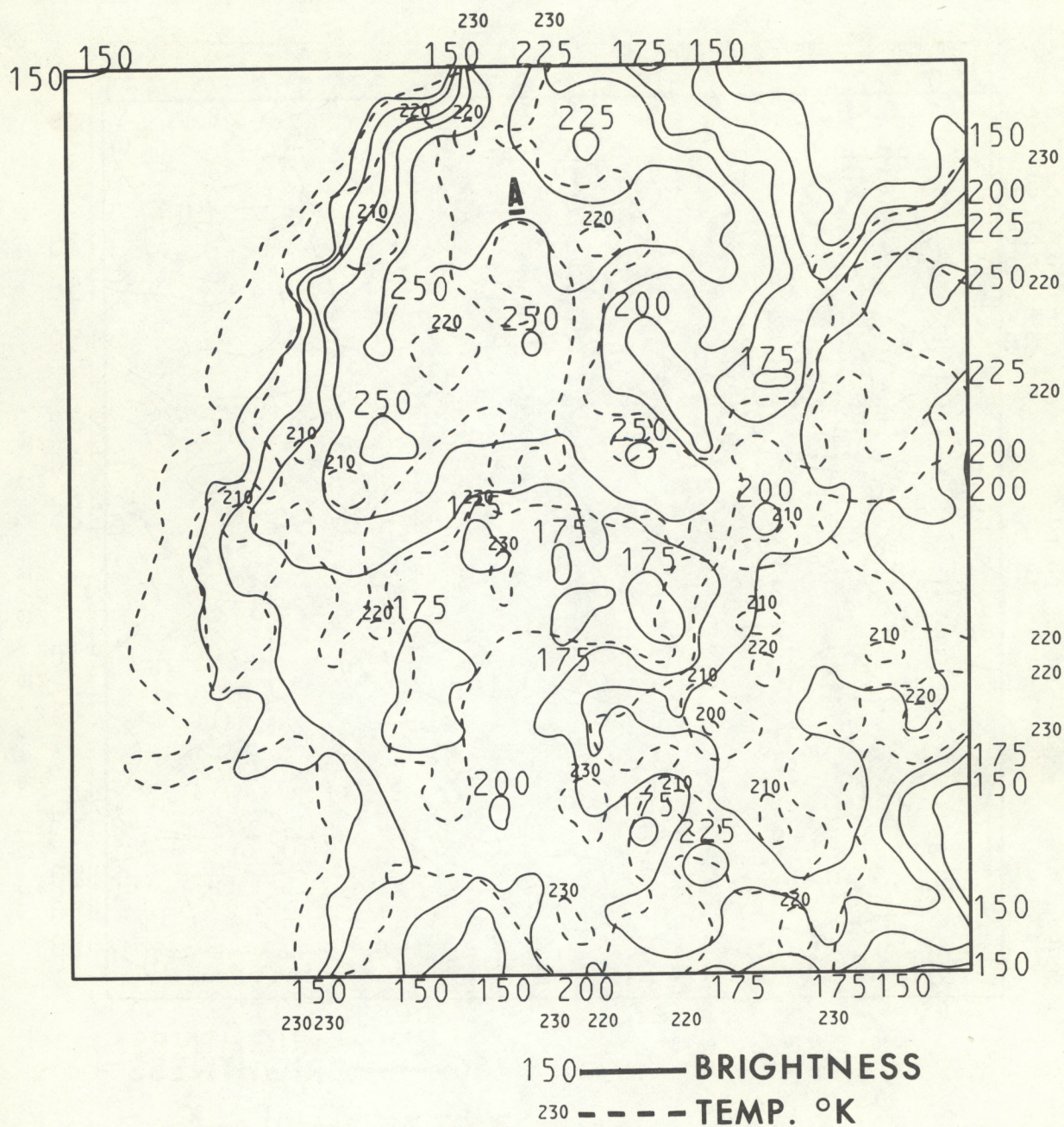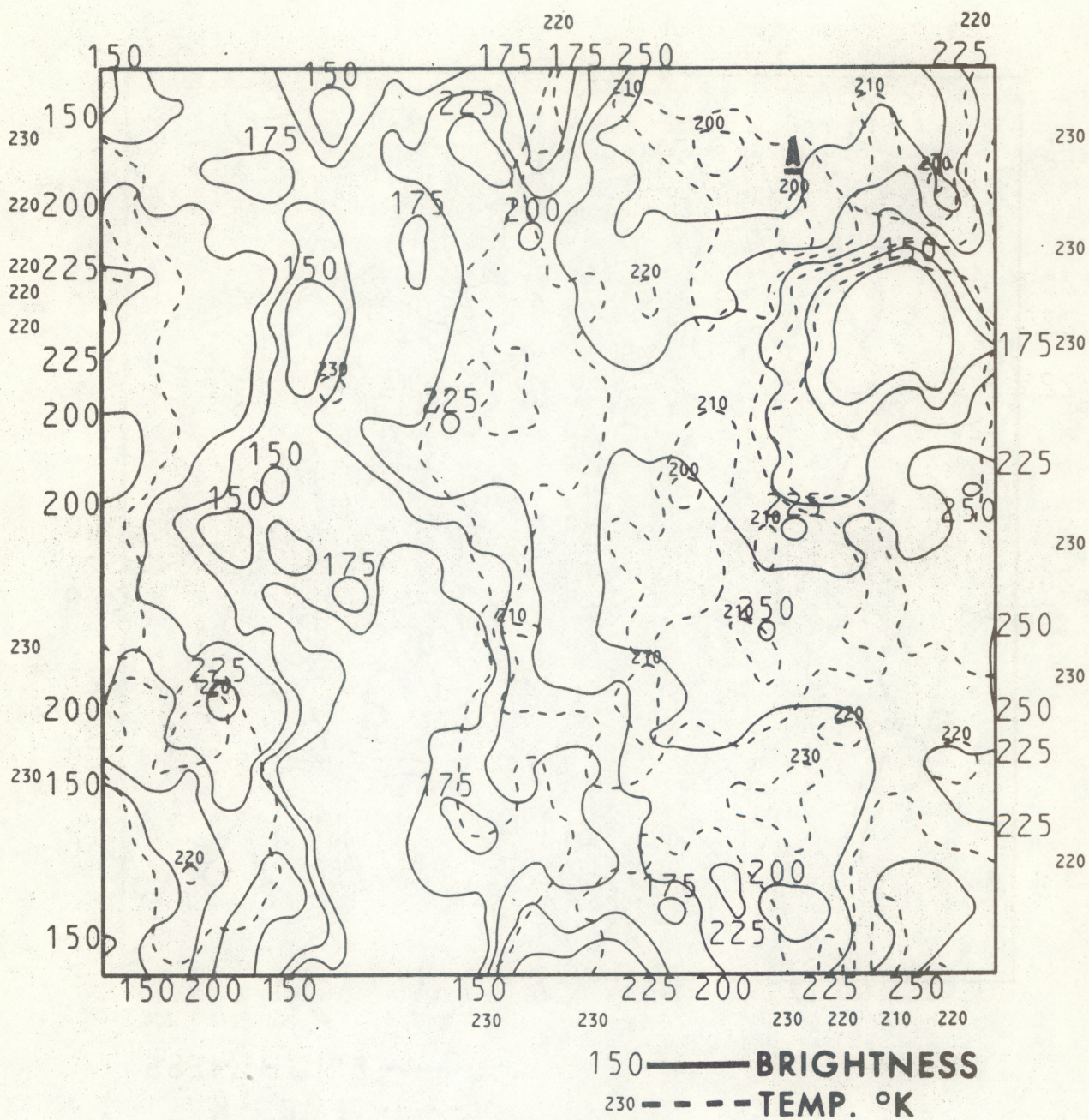and brightness (solid) for location 20-55.

GRID 19-55   JUNE 25, 1971

Figure 9.--Analyzed map of infrared temperatures (dashed)
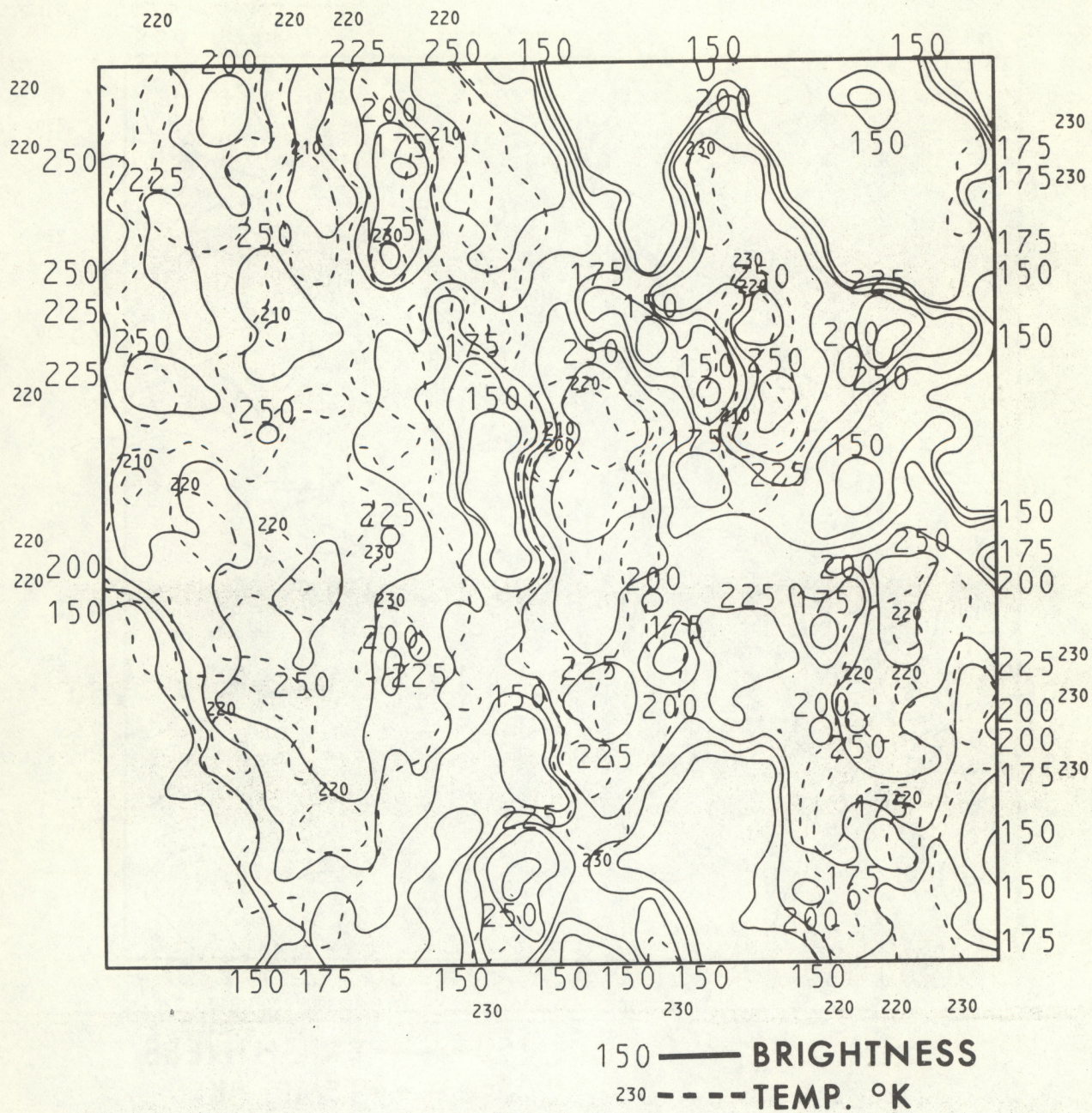and brightness (solid) for location 19-55.

GRID 5-42   JUNE 25, 1971

Figure 10.--Analyzed map of infrared temperatures (dashed)
and brightness (solid) for location 5-42.

GRID 6-42 JUNE 25, 1971

Figure 11.--Analyzed map of infrared temperatures (dashed) and brightness (solid) for location 6-42.

GRID 7-43 JUNE 25, 1971

150 ——— **BRIGHTNESS**
230 - - - - **TEMP. °K**

Figure 12.--Analyzed map of infrared temperatures (dashed)
and brightness (solid) for location 7-43.

NESS 29   The Operational Processing of Solar Proton Monitor and Flat Plate Radiometer Data. Henry L. Phillips and Louis Rubin, May 1972. (COM-72-10719)

NESS 30   Limits on the Accuracy of Infrared Radiation Measurements of Sea-Surface Temperature From a Satellite. Charles Braun, December 1971. (COM-72-10898)

NESS 31   Publications and Final Reports on Contracts and Grants, 1970--NESS. December 1971. (COM-72-10303)

NESS 32   On Reference Levels for Determining Height Profiles From Satellite-Measured Temperature Profiles. Christopher M. Hayden, December 1971. (COM-72-50393)

NESS 33   Use of Satellite Data in East Coast Snowstorm Forecasting. Frances C. Parmenter, February 1972. (COM-72-10482)

NESS 34   Chromium Dioxide Recording--Its Characteristics and Potential for Telemetry. Florence Nesh, March 1972. (COM-72-10644)

NESS 35   Modified Version of the Improved TIROS Operational Satellite (ITOS D-G). A. Schwalb, April 1972. (COM-72-10547)

NESS 36   A Technique for the Analysis and Forecasting of Tropical Cyclone Intensities From Satellite Pictures. Vernon F. Dvorak, June 1972. (COM-72-10840)

NESS 37   Some Preliminary Results of 1971 Aircraft Microwave Measurements of Ice in the Beaufort Sea. Richard J. DeRycke and Alan E. Strong, June 1972. (COM-72-10847)

NESS 38   Publications and Final Reports on Contracts and Grants, 1971--NESS. June 1972. (COM-72-11115)

NESS 39   Operational Procedures for Estimating Wind Vectors From Geostationary Satellite Data. Michael T. Young, Russell C. Doolittle, and Lee M. Mace, July 1972. (COM-72-10910)

NESS 40   Convective Clouds as Tracers of Air Motion. Lester F. Hubert and Andrew Timchalk, August 1972. (COM-72-11421)

NESS 41   Effect of Orbital Inclination and Spin Axis Attitude on Wind Estimates From Photographs by Geosynchronous Satellites. Linwood F. Whitney, Jr., September 1972. (COM-72-11499)

NESS 42   Evaluation of a Technique for the Analysis and Forecasting of Tropical Cyclone Intensities From Satellite Pictures. Carl O. Erickson, September 1972. (COM-72-11472)

NESS 43   Cloud Motions in Baroclinic Zones. Linwood F. Whitney, Jr., October 1972. (COM-73-10029)

NESS 44   Estimation of Average Daily Rainfall From Satellite Cloud Photographs. Walton A. Follansbee, January 1973. (COM-73-10539)

NESS 45   A Technique for the Analysis and Forecasting of Tropical Cyclone Intensities From Satellite Pictures. (Revision of NESS 36) Vernon F. Dvorak, February 1973. (COM-73-10675)

NESS 46   Publications and Final Reports on Contracts and Grants, 1972--NESS. April 1973.

NESS 47   Stratospheric Photochemistry of Ozone and SST Pollution: An Introduction and Survey of Selected Developments Since 1965. Martin S. Longmire, March 1973. (COM-73-10786)

NESS 48   Review of Satellite Measurements of Albedo and Outgoing Long-Wave Radiation. Arnold Gruber, July 1973.

NESS 49   Operational Processing of Solar Proton Monitor Data. Louis Rubin, Henry L. Phillips, and Stanley R. Brown, August 1973.